Reliability of Solid-State Lighting Electrical Drivers Subjected to WHTOL Accelerated Aging

Pradeep Lall [1], Peter Sakalaukus [1], Lynn Davis [2]
[1] Auburn University
NSF-CAVE3 Electronics Research Center
Auburn, AL, USA 36849
[2] RTI International, Research Triangle Park, NC, 27709
Email: lall@auburn.edu
Tele: (334)844-3424

ABSTRACT

An investigation of a solid-state lighting (SSL) luminaire with the focus on the electronic driver which has been exposed to a standard wet hot temperature operating life (WHTOL) of 85% RH and 85°C in order to assess reliability of prolonged exposer to a harsh environment has been conducted. SSL luminaires are beginning introduced as headlamps in some of today's luxury automobiles and may also be fulfilling a variety of important outdoor applications such as overhead street lamps, traffic signals and landscape lighting. SSL luminaires in these environments are almost certain to encounter excessive moisture from humidity and high temperatures for a persistent period of time. The lack of accelerated test methods for LEDs to assess long-term reliability prior to introduction into the marketplace, a need for SSL physics based PHM modeling indicators for assessment and prediction of LED life, as well as the U.S. Department of Energy's R&D roadmap to replace todays lighting with SSL luminaires makes it important to increase the understanding of the reliability of SSL devices, specifically, in harsh environment applications.

In this work, a set of SSL electrical drivers were investigated to determine failure mechanisms that occur during prolonged harsh environment applications. Each driver consists of four aluminum electrolytic capacitors (AECs) of three different types and was considered the weakest component inside the SSL electrical driver. The reliability of the electrical driver was assessed by monitoring the change in capacitance and the change in equivalent series resistance for each AEC, as well as monitoring the luminous flux of the SSL luminaire or the output of the electrical driver. The luminous flux of a pristine SSL electrical driver was also monitored in order to detect minute changes in the electrical drivers output and to aid in the investigation of the SSL luminaires reliability. The failure mechanisms of the electrical drivers have been determined and are presented in this paper.

KEY WORDS: Electrolytic Capacitor, Solid-State Lighting, LED

MOTIVATION

The U.S. Department of Energy (DOE) has made a long-term commitment to advance R&D breakthroughs in efficiency and performance of solid-state lighting (SSL). SSL technology has the potential to reduce the U.S. lighting energy usage in half and produce large savings. The DOE has developed a comprehensive national strategy that encompasses Basic Energy Sciences, Core Technology Research, Product Development, Manufacturing Research and Development (R&D) Initiative, Market Development Support, SSL Partnerships, and Standards Development. [1] The lack of accelerated test methods for LEDs to assess reliability prior to introduction into the marketplace does not exist. There is a need for SSL physics based PHM modeling indicators for assessment and prediction of LED life.

NOMENCLATURE

SSL	Solid-State Lighting
WHTOL	Wet Hot Temperature Operating Life
AEC	Aluminum Electrolytic Capacitor
RH	Relative Humidity
LED	Light Emitting Diode
ESR	Equivalent Series Resistance
CAP	Capacitance
PWM	Pulse-Width Modulation
LCR	Inductance, Capacitance and Resistance
T_o	Operating Temperature
V_o	Operating Voltage
C_o	Operating Capacitance
$\Phi_{test}(\lambda)$	Corrected Spectral Radiant Flux
$\Phi_m(\lambda)$	Measured Spectral Radiant Flux
α_{CCF}	Absorption Correction Factor
Φ_{test}	Luminous Flux
$V(\lambda)$	Spectral Luminous Efficiency Function
K_m	Maximum Spectral Luminous Efficacy

INTRODUCTION

Luminaires are beginning to replace today's incandescent light bulbs and are becoming more prevalent in everyday applications. SSL luminaires are beginning introduced as headlamps in some of today's luxury automobiles and may also be fulfilling a variety of important outdoor applications such as overhead street lamps, traffic signals and landscape lighting. SSL luminaires in these environments are almost certain to encounter excessive moisture ingress from humidity

and high temperatures for a persistent period of time. Luminaires subjected to WHTOL for a prolonged period of time may see premature failure of the individual components, such as an aluminum electrolytic capacitor (AEC). AEC degradation may cause the electrical drivers to fail completely due to a current surge or produce an undesirable light output of the light emitting diodes (LEDs). This can potentially erode a manufactures profit margin due to warrantied replacement of the luminaire. AECs are typically considered the "weakest link" inside of an electrical driver compared to the other components. Therefore, they were directly monitored in this work to aid in understanding the reliability of the SSL luminaire.

An AEC is a type of capacitor that uses an electrolyte to achieve a larger capacitance per unit volume compared to traditional capacitors. They are used in high current and low frequency electrical circuits, such as an LED electrical driver, and are needed to help convert AC power to DC power [2]. An AEC is composed of a cathode aluminum foil, electrolytic paper, liquid electrolyte and a dielectric [3] – [4]. The capacitance can be calculated by knowing the dielectric constant, surface area of the dielectric and the thickness of the dielectric [3] – [5]. The ESR can be found by summing the electrolytic resistance, dielectric loss and the electrode resistance using equations outlined in the literature [3], [6] – [7]. In this work, the ESR and capacitance (CAP) were measured directly using a handheld LCR meter.

The predominant failure mechanism of the AEC is the loss of the liquid electrolyte through dissipation and decomposition. Liquid electrolyte loss can be attributed to an elevated ambient temperature, electrochemical reactions at the dielectric layer, moisture ingress or diffusion through the seal [6] – [5]. This will lead to a drift of the electrical parameters of the AEC (i.e. CAP and ESR). If an AEC is kept at an elevated ambient temperature for a prolonged period of time causing liquid electrolyte degradation, then the capacitance will decrease and the ESR will increase [3] – [14]. Therefore, this makes CAP and ESR excellent leading indicators to monitor the health of an AEC. This along with the luminous flux or light output of the LED gives great insight on the health of the entire luminaire system. In this work, the ESR and CAP have been measured directly for AECs subjected to a WHTOL testing of 85 °C/85% RH. The luminous flux of the SSL luminaire was determined using the IES LM-79-08 testing standards to investigate changes in the output of the electrical driver. The failure mechanisms, as well as the failure modes of the electrical drivers have been determined and are presented in this paper.

TEST VEHICLE

The test vehicle for this work was an off-the-shelf luminaire which consisted of a LED downlight module, an electrical driver (boost PWM half-bridge rectifier) and wired connections to attach the two components and to connect the electrical driver to the main power supply. A single light engine was used in all the tests. However, the driver powering the light engine was changed out as described below. This approach facilitates assignment of any observed changes in lumen maintenance of the driver. The luminaire shown in Figure 1 illustrates how each component of the system is incorporated. A base line luminous flux value was obtained using an untested electrical driver during each time step. The pristine value was used as a comparison to the luminous flux values found for each electrical driver under WHTOL in order to investigate minute changes in the lumen maintenance.

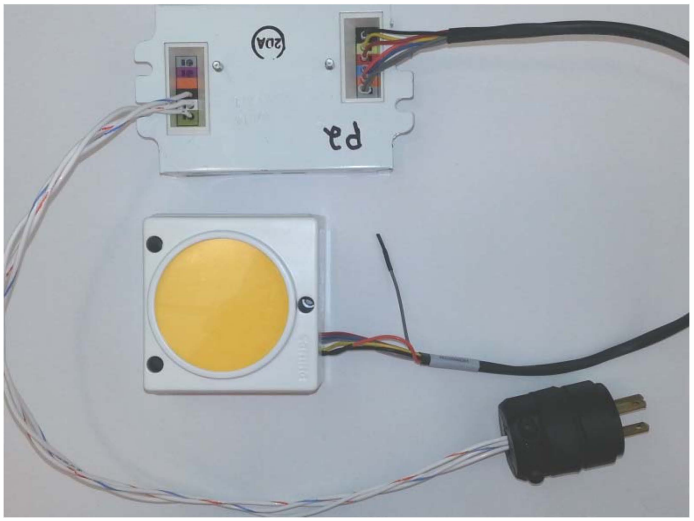

Figure 1: The Luminaire System.

Ten sample sets consisting of four AECs were used in this experiment. Each sample set was taken from a separate, single electrical driver. These AECs were removed to directly measure the CAP and ESR. Figure 2 depicts the circuit board of a single electrical driver with the four AECs removed.

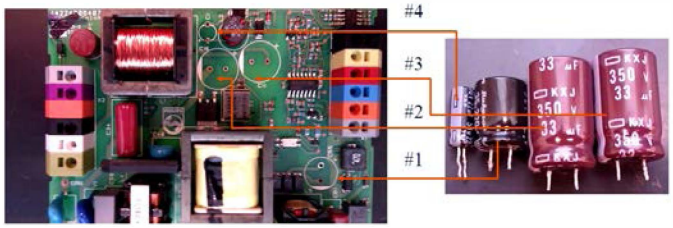

Figure 2: AECs Removed from the Electrical Driver.

Each electrical driver consisted of four AECs of three different types. The AEC characteristics are given in Table 1.

Table 1: AEC Characteristics.

AEC #	Endurance [Hrs.]	T_o [°C]	V_o [Vdc]	C_o [µF]
1	8000 to 10000	-40 to +105	35	220
2	10000 to 12000	-40 to +105	350	33
3	10000 to 12000	-40 to +105	350	33
4	4000 to 5000	-40 to +105	50	22

TEST ENVIRONMENT

The removed AECs and the remaining portion of the electrical driver were kept in a Thermotron humidity chamber at 85 °C/85% RH for the duration of the test. The components were removed from the chamber and allowed to cool to room temperature for approximately one hour before measurements were taken. The ESR and CAP of each AEC were measured directly using an Agilent U1733C handheld LCR meter. See Figure 3 below.

Figure 3: Agilent U1733C LCR Meter (Courtesy of Agilent).

Luminous flux calculations were also carried out for each sample set on the same pristine light engine following the IES LM-79-08 standard [15]. The AECs were connected to its corresponding electrical driver through a bread board. The light output leads of the electrical driver were connected to another portion of the bread board which allowed easy switching between electrical drivers to record the radiant flux values needed to calculate the luminous flux. An USB4000 Spectrometer from Ocean Optics, SpectraSuite software and a one meter integrating sphere were used to accurately obtain the radiant flux data of the downlight for each driver. Figure 4 illustrates the luminous flux setup.

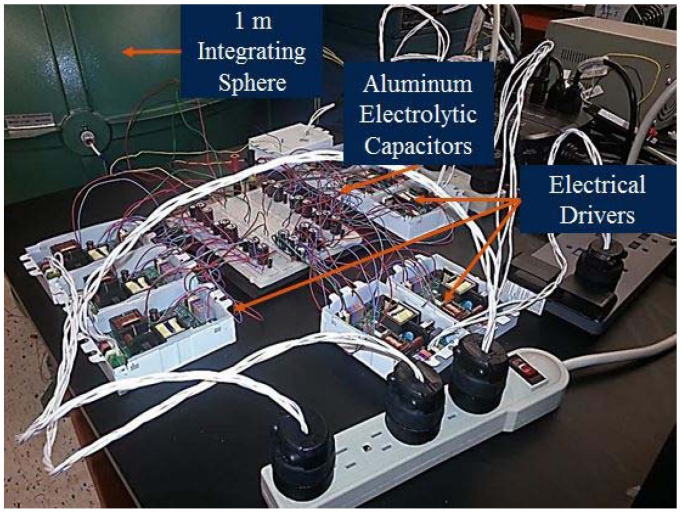

Figure 4: Luminous Flux Measurement Setup.

IES LM-79-08 TEST STANDARD

The total spectral radiant flux, $\Phi_{test}(\lambda)$, of a SSL product under test is obtained by comparison to the total spectral radiant flux of a reference standard [15]. It can be found using the following equation:

$$\Phi_{test}(\lambda) = \Phi_{m}(\lambda) \cdot \alpha_{CCF} \quad (1)$$

The measured spectral radiant flux, $\Phi_m(\lambda)$, of the test lamp is computed using the SpectraSuite software. The self-absorption factor, α_{CCF}, can be found through a comparison of an auxiliary lamp measurement with the test lamp inside the integrating sphere and an auxiliary lamp measurement with the calibration lamp standard inside the sphere. Both the test lamp and calibration lamp standard are off during the auxiliary measurements. This is a critical parameter since SSL products have a different physical size and shape compared to the calibration lamp standard used to calibrate the integrating sphere and the spectrometer. The ratio of the measurements of the auxiliary lamp with the reference lamp divided by the auxiliary lamp with the test lamp will produce the self-absorption factor. The total luminous flux, Φ_{test}, in lumens [lm] of the SSL product under test can now be found using the total spectral radiant flux found from equation (1) with equation (2) [15].

$$\Phi_{test} = K_m \cdot \int_{380}^{780} \Phi_{test}(\lambda) \cdot V(\lambda) \cdot d\lambda \quad (2)$$

$$K_m = 683\,lm/W$$

The spectral luminous efficiency function for photopic vision, $V(\lambda)$, is well documented in literature and K_m is the maximum spectral luminous efficacy [16].

RESULTS

WHTOL testing was conducted on ten electrical drivers until failure was reached. The CAP and ESR of the AECs were measured at each test interval along with the luminous flux associated with each electrical driver. The luminous flux for each electrical driver never deviated outside of the pristine range given by the manufacturer through the course of the experiment. Luminous flux proved not to be a precursor for describing the degradation of these electrical drivers under WHTOL testing. Each electrical driver was tested until a failure mechanism was present. Each electrical driver had a different failure time with the last failure occurring at 3635.37 hours. Figure 5 shows the relative luminous flux values (measured value divided by original value) over the course of WHTOL accelerated testing for all ten electrical drivers.

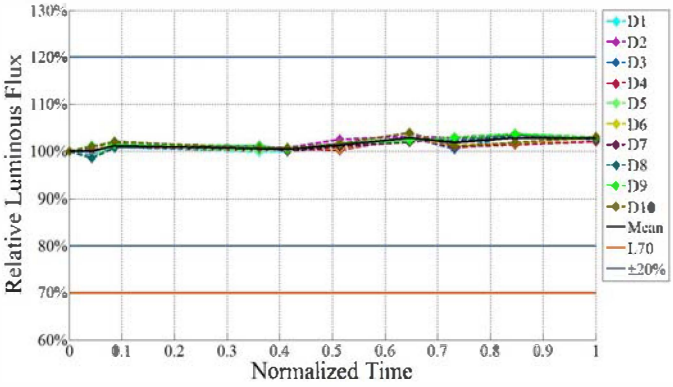

Figure 5: Relative Luminous Flux with Pristine Bounds.

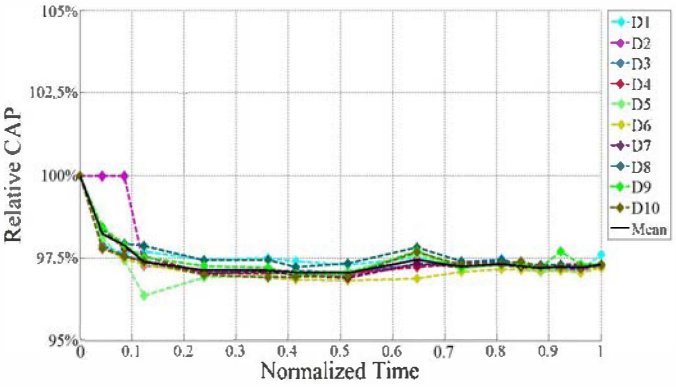

Figure 6: Relative CAP of AEC 1.

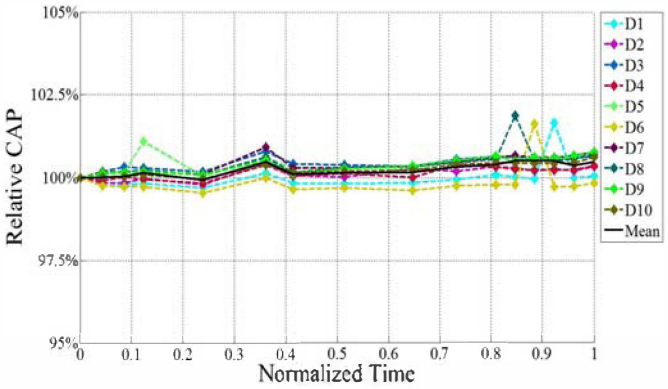

Figure 7: Relative CAP of AEC 2.

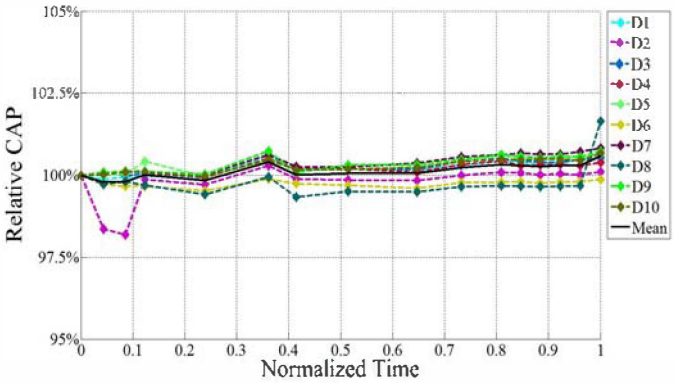

Figure 8: Relative CAP of AEC 3.

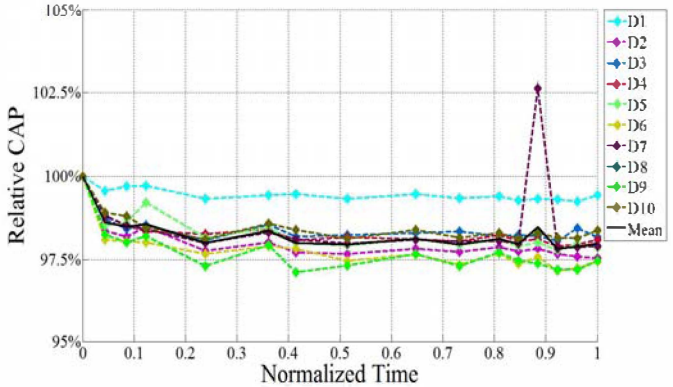

Figure 9: Relative CAP of AEC 4.

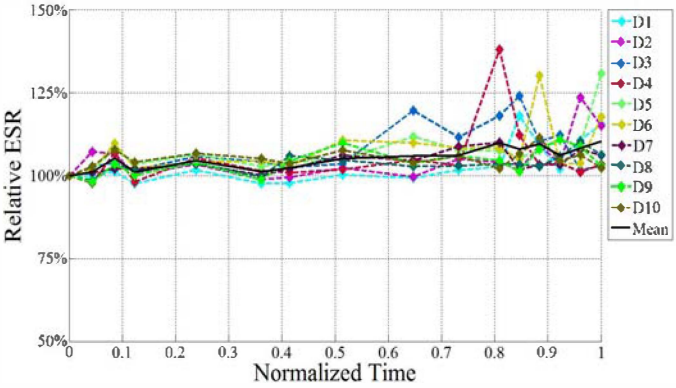

Figure 10: Relative ESR of AEC 1.

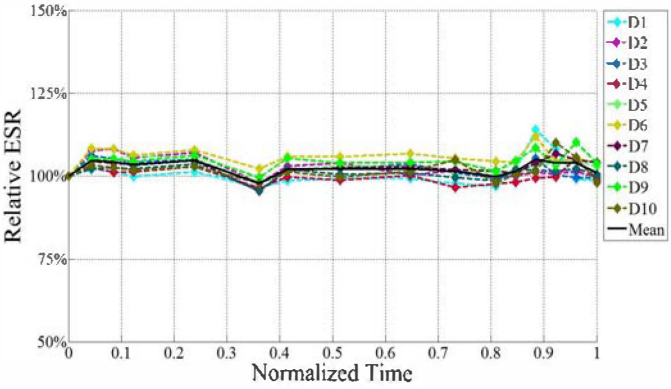

Figure 11: Relative of ESR AEC 2.

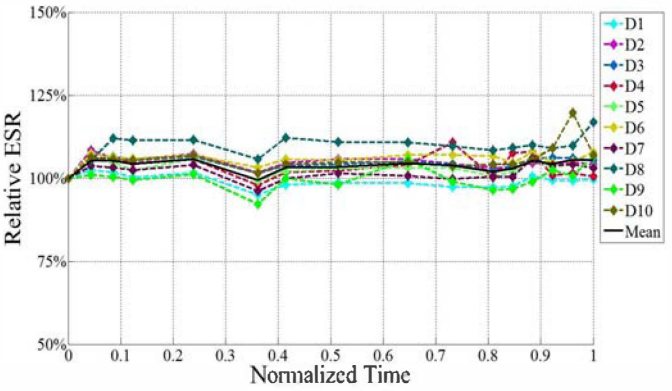

Figure 12: Relative ESR of AEC 3.

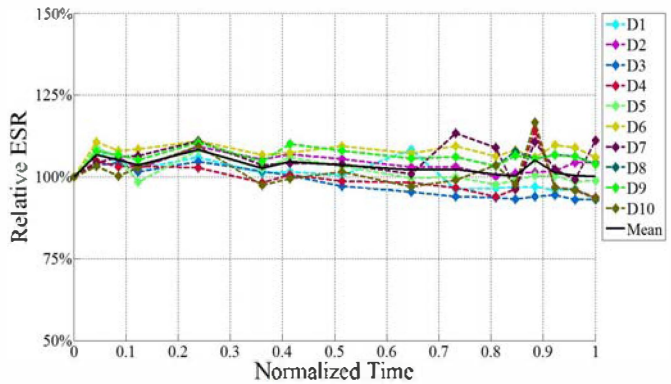

Figure 13: Relative ESR of AEC 4.

The CAP and ESR also did not forecast the degradation of the electrical drivers. Once the electrical drivers failed, the AECs were placed back into WHTOL testing to investigate further. The CAP and ESR values were measured at regular intervals of one week with testing completely stopped at 4294.43 hours. The relative CAP and relative ESR for the four AECs inside the electrical drivers are shown in Figure 6 – Figure 13. The ten electrical drivers did experience component level failure which rendered each electrical driver useless to some degree. Multiple failure mechanisms have been found for this luminaire with each electrical driver experiencing only one of the failure mechanisms. Table 2 catalogs the failure mechanisms and failure modes of each electrical driver.

Table 2: Failures under WHTOL Testing.

Driver	T_f [hrs.]	Failure Mechanism	Failure Mode
# 1	333.37	IGBT/MOSFET	Open Circuit
# 2	0.00	Unknown	Open Circuit
# 3	3143.78	CL21-S PFCAP	CAP Leakage
# 4	3635.37	CL21-S PFCAP	CAP Leakage
# 5	0.00	SMD-R 1206	Open Circuit
# 6	3635.37	CL21-S PFCAP	CAP Leakage
# 7	369.12	IGBT/MOSFET	Open Circuit
# 8	185.15	SMD-C 1206	Open Circuit
# 9	369.12	IGBT/MOSFET	Open Circuit
# 10	3635.37	CL21-S PFCAP	CAP Leakage

(a)

(b)

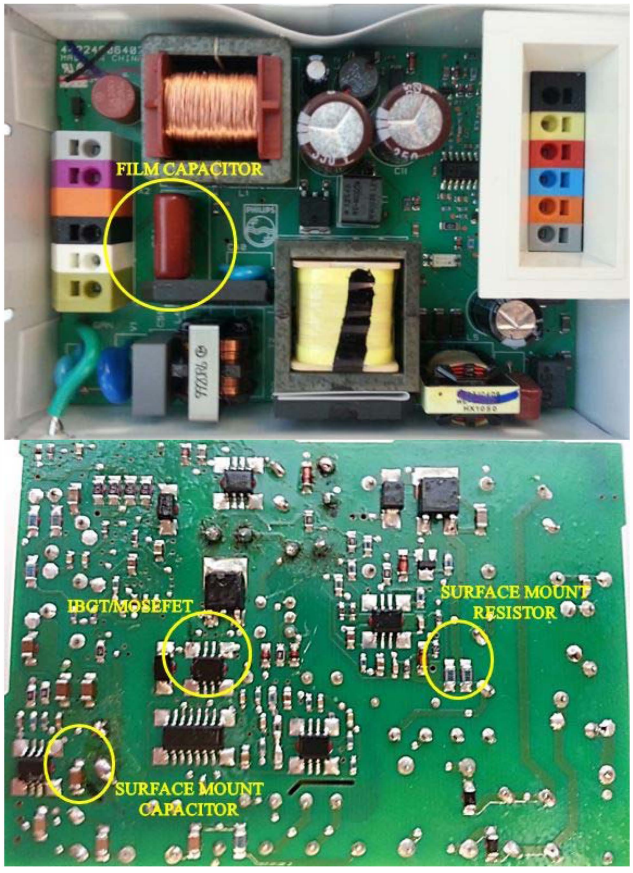

Figure 14: Identification of Failure Mechanisms for WHTOL Testing: (a) Top (b) Bottom.

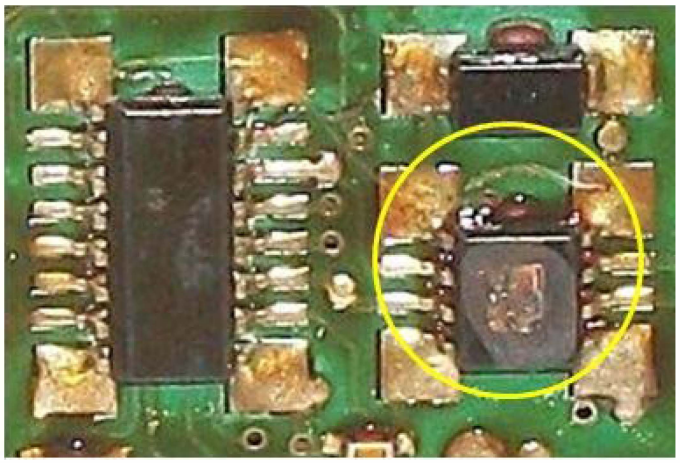

Figure 15: Failure Mechanism of WHTOL Driver One.

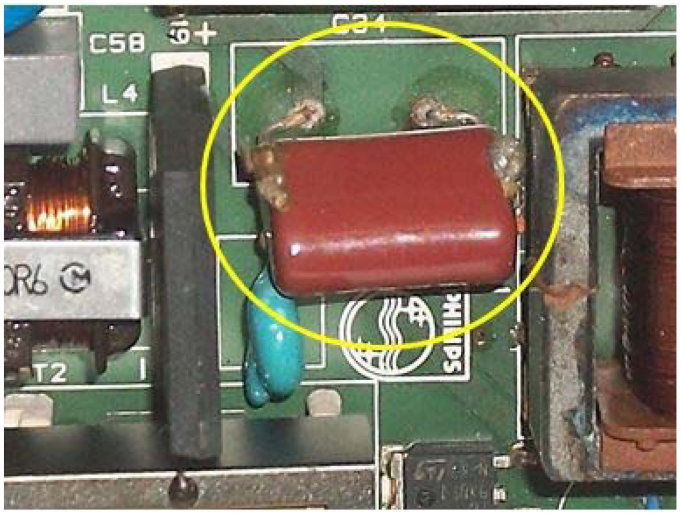

Figure 16: Failure Mechanism of WHTOL Driver Three.

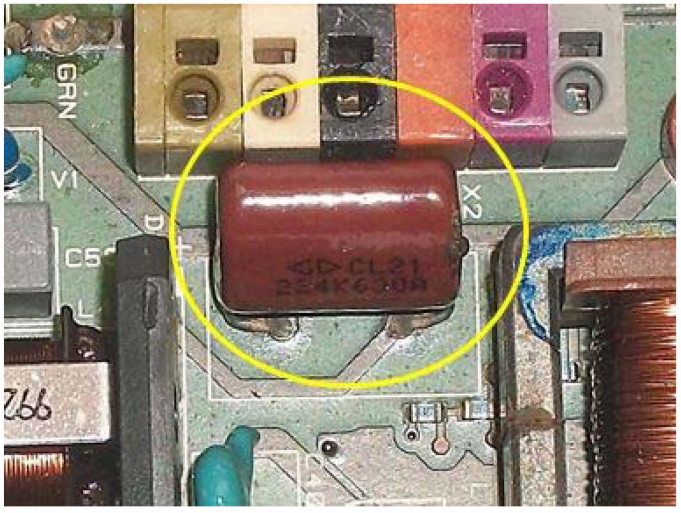

Figure 17: Failure Mechanism of WHTOL Driver Four.

Figure 14 depicts a pristine electrical driver from the top and bottom views to show the placement of each failed component. The different failure mechanisms listed in Table 2 have been circled to show the components in their pristine form and their location inside the electrical driver. The failed components of each electrical driver under WHTOL are

shown below except for driver two. There was no visible damage to this driver even though it wouldn't power on.

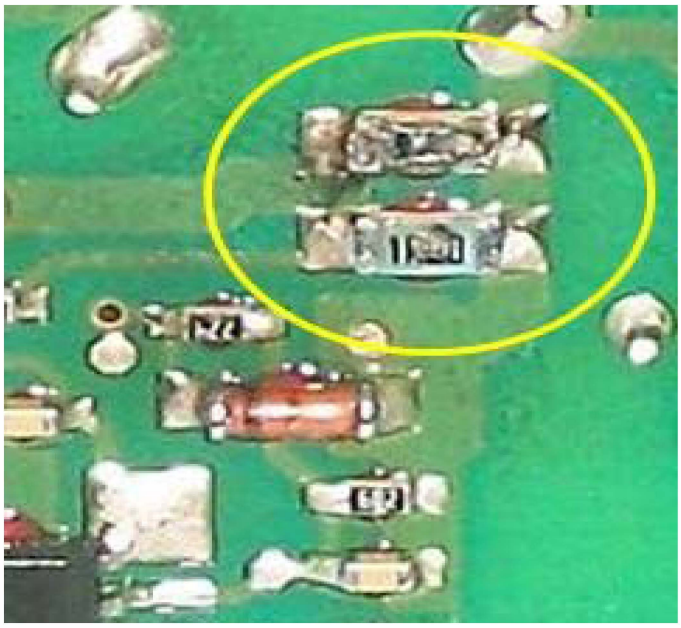

Figure 18: Failure Mechanism of WHTOL Driver Five.

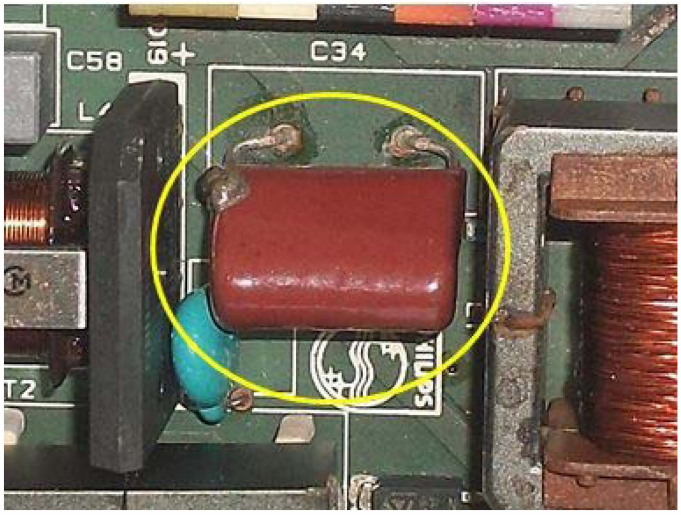

Figure 19: Failure Mechanism of WHTOL Driver Six.

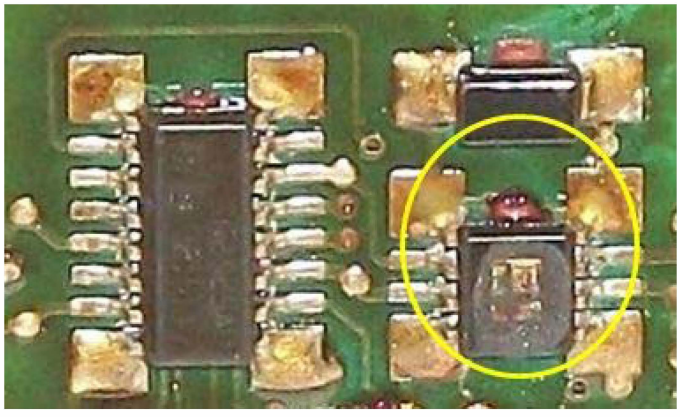

Figure 20: Failure Mechanism of WHTOL Driver Seven.

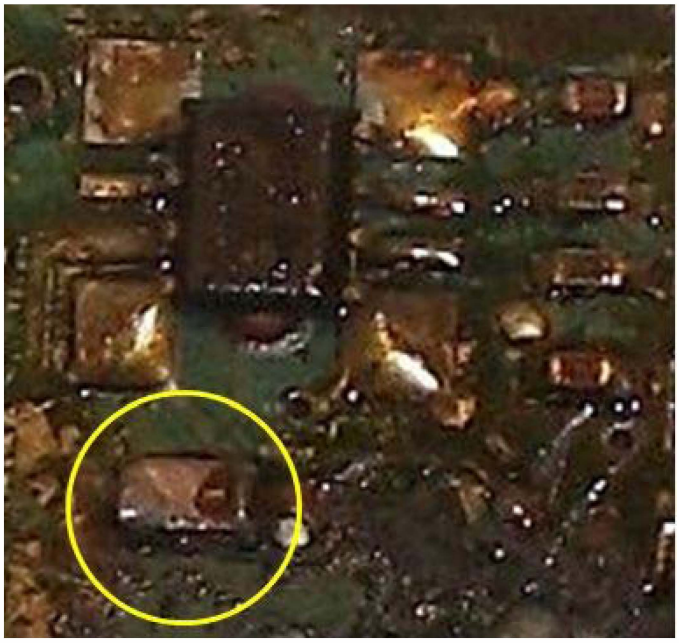

Figure 21: Failure Mechanism of WHTOL Driver Eight.

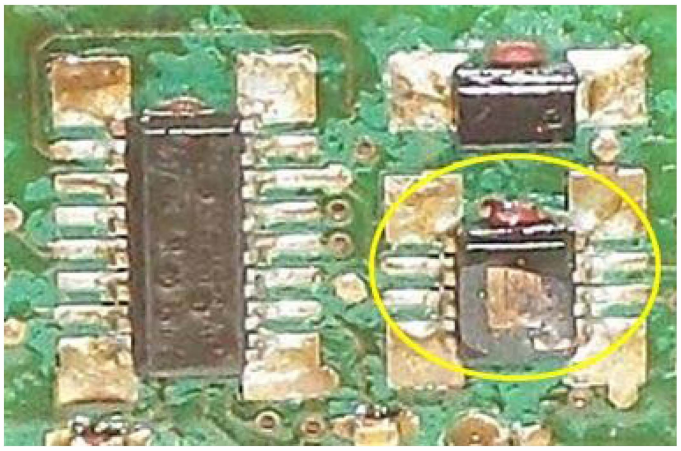

Figure 22: Failure Mechanism of WHTOL Driver Nine.

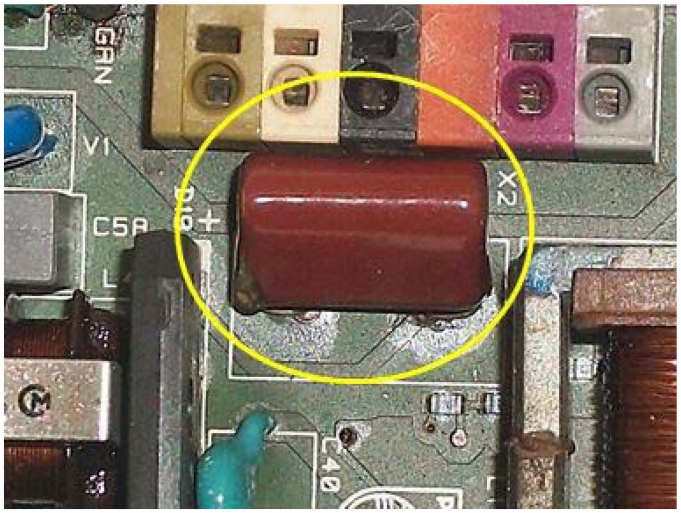

Figure 23: Failure Mechanism of WHTOL Driver Ten.

SUMMARY & CONCLUSIONS

This paper has shown an investigation of an off the shelf luminaire system with the focus on the electronic drivers. Specific components inside the electrical driver, the AEC, were monitored as possible precursors of failure. The electrical drivers were aged using a life test of 85°C/85% RH. The four AECs of three different types inside each electronic driver were removed from the driver to obtain the exact CAP and ESR values using a handheld LCR meter. To monitor the overall health of the luminaire, the luminous flux was measured for each electrical driver under test using the same pristine lamp.

It was hypothesized that the AECs would be the "weakest link" of the electrical driver and a suitable leading indication of failure well before failure occurred. Also, the luminous flux was monitored as a possible indication of the overall health of the electrical driver. The measured parameters proved not to be an indication of failure for these electrical drivers. The CAP and luminous flux never deviated outside of the pristine range and the ESR did not deviate much from its original measurement. The parameters did not give any indication the system was going to fail. There were two predominate, failure mechanisms observed during the duration of testing which comprised 70% of the test vehicles. One predominate, failure mechanism was the CL21 series polyester film capacitor located on the topside the electrical driver. This film capacitor started spewing the internal material and smoking. The electrical driver was still functional and powered the light engine normally. It was deemed failed because of health and safety concerns due to the possible toxic nature of the internal material. The other predominate, failure mechanism was an IGBT/MOSFET located on the undercarriage of the electrical driver. In this case, the top of the IGBT/MOSFET was blown off causing catastrophic failure to the system and was likely due to an electrical surge from moisture seepage into the component. Neither one of the observed, failure mechanisms overlapped meaning each test vehicle experienced one specific failure mechanism. Only two failure modes were present during the WHTOL testing: an open circuit/no light and capacitance degradation.

ACKNOWLEDGMENTS

The work presented here in this paper has been supported by a research grant from the Department of Energy under Award Number DE-EE0005124.

REFERENCES

[1] U.S. Department of Energy: Energy Efficiency & Renewable Energy. "Solid-State Lighting." *Building Technology Programs.* DOE, 9 April 2012. Web. 5 May 2012.

[2] Georgiev, Alexander M. *The Electrolytic Capacitor.* New York: Murray Hill Books, 1945.

[3] Rubycon Corporation, *Technical Notes for Electrolytic Capacitor*.

[4] Nichicon Inc. *General Descriptions of Aluminum Electrolytic Capacitors.* 2002.

[5] Jianghai Europe GmbH. *Electrolytic Capacitor Lifetime Estimation.* 2010.

[6] Han, L. and Narendran, N. "Developing an Accelerated Life Test Method for LED Drivers." *Proc. of SPIE: 9th International Conference on Solid State Lighting.* 2009.

[7] Harada, K., Katsuki, A. and Fujiwara, M. "Use of ESR for Deterioration Diagnosis of Electrolytic Capacitor." *IEEE Trans. on Power Electronics.* Vol. 8, pp. 355-361, Oct., 1993.

[8] Gasperi, M.L. "Life Prediction Model for Aluminum Electrolytic Capacitors." *IEEE Industry Applications Conf.* Vol. 3, pp. 1347-1351, Oct., 1996.

[9] BHC Components. *Aluminum Electrolytic Capacitor Application Notes*. 2002.

[10] Sankaran, V.A., Rees, F.L., and Avant, C.S. "Electrolytic Capacitor Life Testing and Prediction." *IEEE Industry Applications Conf.* Vol. 2, pp. 1058-1065, Oct., 1997.

[11] Stevens, J.L., Shaffer, J.S. and Vandenham, J.T. "The Service Life of Large Aluminum Electrolytic Capacitors: Effects of Construction and Application." *IEEE Trans. on Industry Applications.* Vol. 38, Issue 5, pp. 1441-1446, Oct. 2002.

[12] Panasonic Industrial Company. *Aluminum Electrolytic Capacitors*. 2008.

[13] Cornell Dubilier Electronics Inc. *Application Guide, Aluminum Electrolytic Capacitors.* 2000.

[14] Celaya, J.R., Kulkarni, C., Biswas, G., Saha, S. and Goebel, K. "A Model-based Prognostics Methodology for Electrolytic Capacitors Based on Electrical Overstress Accelerated Aging." *Annual Conf. of the PHM Society.* 2011.

[15] IES Illuminating Engineering Society. *IES LM-79-08 Approved Method: Electrical and Photometric Measurements of Solid-State Lighting Products.* 2008.

[16] DeCusatis, Casimer. *Handbook of Applied Photometry.* New York: AIP Press, 1997.